

Punching Shear Resistance of Flat Slabs By Shear Heads

*Mohamed Badawy¹, Mohamed Saafan², Sherif Elwan³, Sherif Elzeiny⁴,
Amr Abdelrahman⁵

¹Research Assistant, Structural Engineering Department., Ain Shams University, Cairo, EGYPT

²Lecturer, Structural Engineering Department, Ain Shams University, Cairo, EGYPT

³Associate Professor, Department of Civil Eng., The Higher Institute of Engineering,
El Sherouk City, Cairo, EGYPT

⁴Professor of Reinforced Concrete Structures, Housing and Building National Research Center, Cairo, EGYPT

⁵Professor, Concrete Engineering Department, Ain shams university, Cairo, EGYPT

Corresponding author: *Mohamed Badawy

ABSTRACT: This paper aims to examine the punching shear resistance of reinforced concrete flat slabs with shear heads. The ACI 318-M (2005), allowed the arrangements of shear heads as one possible alternative of punching shear reinforcement. In this study, seven half- scale reinforced concrete flat slabs divided into two groups were casted and tested. The first group deals with testing three specimens of flat slabs connected with square columns, one specimen without any shear head and the other two specimens reinforced by steel shear head sections with lengths equal to 1.75h and 2.25h, respectively from column face. The second group deals with four specimens of flat slabs connected with rectangular columns. one specimen without any shear head and the other three specimens reinforced by steel shear head sections with length equal to 1.75h with two cut ends at angles 90 and 45 degrees, and the last one with length equal to 2.25h. All specimens were loaded until failure. The first punching crack load, ultimate load, deformation, punching perimeter, strain in steel bars, strains in steel shear head sections and failure mechanisms of each specimen were generated and analyzed. The results show that shear head reinforcement moves punching perimeter away from column face and accordingly increase punching shear capacity of flat slabs. Based on the experimental results, a simple process has been proposed to predict the improvement of load carrying capacity and punching failure load of flat slabs with shear heads and compared these results with different code values. The theoretical prediction values were then compared with the experimental data and good agreement was found.

Keywords: Punching shear; flat slabs; shear heads; punching shear reinforcement; punching perimeter; punching failure load.

Date of Submission: 09 -11-2017

Date of acceptance: 28-11-2017

I. INTRODUCTION

The flat slabs are widely used in construction; in this type of structures the punching shear is one of the main design criteria due to its brittle failure nature. The application of punching shear reinforcement as a technique for improving punching shear capacity of reinforced concrete flat slabs have been widely used in recent years. Such technique is relatively easy to apply in comparison to conventional methods. A large discussion about the using of the shear reinforcements such that bent-up bars, closed stirrups, open stirrups, continuous stirrups, inclined stirrups, shear hoops, stud rails and double headed studs has been made in many thesis. Figure (1) shows different techniques of shear reinforcement in flat slabs. The common agreement is that the failure can be divided in four large categories: flexural failure by yielding of steel reinforcement at tension, peak shear capacity, failure inside the shear reinforcement area and failure outside the shear reinforced area.

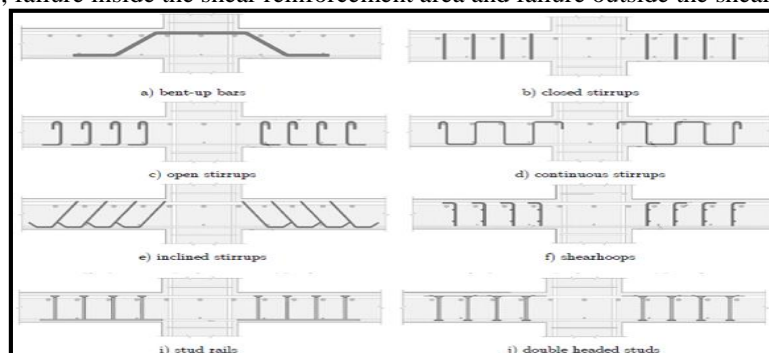


Figure (1) Different techniques of shear reinforcement in flat slabs.

Luca et al. (2011), developed 7 full-scale specimens (3000×3000×250 mm) reproducing the support region of an actual flat slab with different layout of bent-up bars are presented. The tests show different potential failure modes and allow understanding the contribution of this reinforcement to the shear-carrying capacity of the specimens. The significant conclusion is that the strength and deformation capacity of slabs with bent up bars compared to slabs without bent-up bars can be significantly increased (Additionally, the flexural reinforcement can be decreased without losing punching strength, which leads to an even larger increase of the deformation capacity and punching failure modes may have developed.

Dan et al. (2011), tested two of the slabs have been provided with stirrup beams, Stirrups beams was made of $\Phi 10$ stirrups forming a beam of 500 mm. Longitudinal bars used to connect stirrups were $4\Phi 10$. $\Phi 10$ hooks connected on $2\Phi 10$ at the edges were used for the diagonal shear reinforcement. The entire “stirrup beam” was position in between the two faces of flexural reinforcement. The results indicated that flat slab column connections with thin slabs and high shear reinforced ratio develop strong flexural behavior failing in flexure. None of the shear reinforced connections reached the maximum punching capacity predicted by any design codes. Specimens reinforced with stirrup beams showing better ductility behavior. Load-deflection behavior was mainly influenced by the type of shear reinforcement than the concrete strength.

Dan et al. (2011), also tested two of flat slabs provided with Double headed stud-rails, reinforcement type II, were welded on a rectangular plate of 20 mm x 3 mm cross-section. The head of the studs was $\Phi 24$ and the welded plate was placed on the tensioned face of the slab. The geometrical configuration of the slab was chosen in order to fit the standard requirements. Square shaped flat slabs had the dimensions of 1500 mm. The nominal height of the slab was 170 mm and the average effective depth 155 mm. Column had square cross section of 300 mm and a height of 600 mm. Slabs were reinforced on both faces with $\Phi 10@100$ mm spacing for tension and integrity.

Columns had 8 bars $\Phi 14$ at each corner and middle point of the four faces and were transversally reinforced with $\Phi 8$ stirrups posed at 100mm. All connections were uniformly supported on rubber bearings along the four sides at an average distance of 30 mm from the edges. This study presents a failure analysis upon four shear reinforced flat slab column connections with thin plates. tension reinforcement ratio was 0.5%. Five perimeters of shear reinforcement, $\Phi 10@100$ mm, under star direction were fitted in the critical perimeter. Average effective depth of the slab was 155 mm and designed concrete strength was C20/25. The results showed that the concrete uniaxial compressive strength does not influence the final failure values. Load-deflection behavior was mainly influenced by the type of shear reinforcement than the concrete strength. Bond conditions and anchorage length highly influence the effectiveness of double headed stud-rails reinforcement. Specimens reinforced with stirrup beams showed rotations 50% smaller that the compared ones, stud-rails showing better ductility behavior.

The ACI 318 code provisions for shear head reinforcement, which have been updated very little since 1977 (ACI Committee 318-1977), are used in conjunction with current and previous research findings (Corley and Hawkins 1968; Hawkins 1974; Hawkins and Corley 1974) to develop the empirical strength model for the connections proposed in this study.

A detailed shear head system was developed by Corley and Hawkins, (1968). This system uses structural steel sections welded together to form a grid which can then be placed around or through a column as shown in Figure (2) Their study formed the basis of the shear head reinforcement design guidance in the American Code Institute design code ACI 318 (ACI-318 M, 2005) and (ACI 318-2011). A total of 21 specimens with the above shear head system (or without any shear head reinforcement) were tested and three typical failure modes (no shear head, over-reinforcing and under-reinforcing) were detected in their experimental study.

The failure surface of the slab without a shear head extended from the intersection of the column face and the compression face of the slab, towards the tension face of the slab with an inclined angle of about (20-30) degree to the horizontal until it reached the tension reinforcement level. This failure mode is depicted in Figure (3) (a).

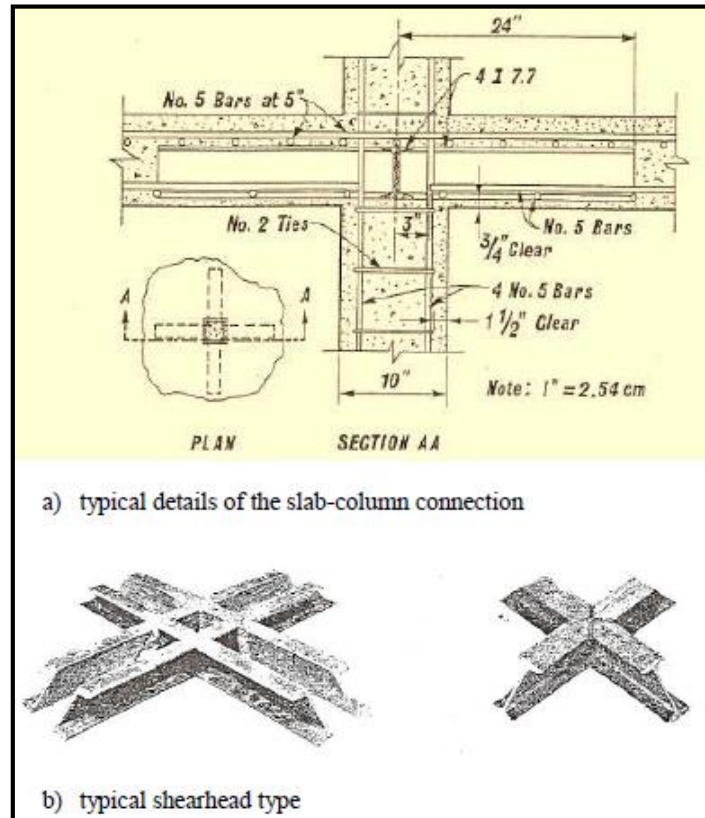


Figure (2): Shear head reinforcement developed by Corley and Hawkins (Corley and Hawkins, 1968).

The failure surface of the slabs containing very heavy shear heads developed from the outer perimeter of the shear head system if the flexural capacity of the shear head at the face of the column was not exceeded. The inclined angle of the failure surface varied from around 20 to 45 degree to the horizontal. This kind of failure was defined as over-reinforcing in the study and Figure (3) (b) shows a typical such failure perimeter. For the specimens with light shear head, the failure surface started from inside the shear head system because the flexural capacity of the shear arm was exceeded. The inclination of the failure face was around 30 degrees to the horizontal. This kind of failures was defined as under-reinforcing in their study, and Figure (3) (c) shows one of such failure perimeters.

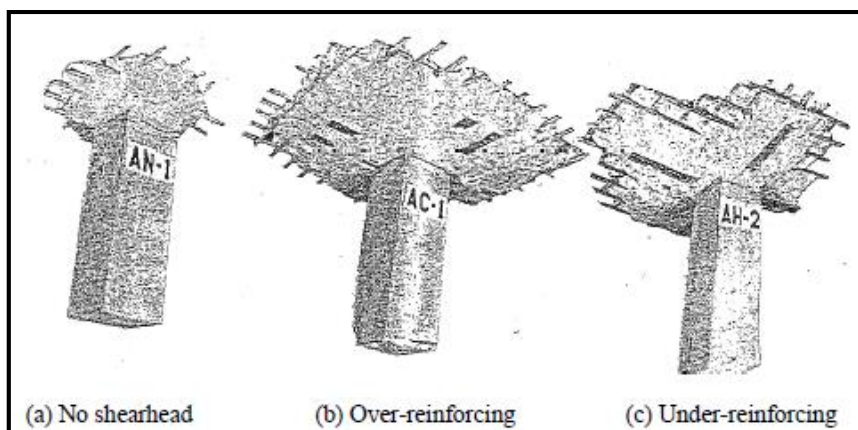


Figure (3): Typical failure modes of flat slab without or with shear head reinforcement (Corley and Hawkins, 1968).

The test results in this study indicated that the slabs with under-reinforcing shear heads failed at a shear stress on a critical section at the end of the shear head reinforcement less than 4, and the use of over-reinforcing shear heads brought the shear strength back to about 4. Based on this conclusion from Corley and Hawkins (1968), a conservative design method for this shear head system in flat slabs was developed and adopted in ACI (ACI 318R-14).

The shear head system developed by Corley and Hawkins (1968) was for reinforced concrete columns. However, it could be adapted for columns with different aspect ratio by connecting the steel shear arms to the columns. This will form the basis of the shear head system used in this research.

II. TESTING PROGRAM

This section describes the experimental work performed through this study beginning with the used materials, specimen's details, measurement devices, test setup, and specimen's grouping.

2.1. Materials Used

Ordinary locally available concrete constituent materials have been used to manufacture the test specimens. All specimens are made from one concrete mix with the proportion shown in Table 1. The target standard 28-days compressive cube strength $f_{cu} = 25\text{MPa}$, and according to the EN the equivalent compressive cylinder strength, $f_c' = 20\text{MPa}$. The results of testing cubes have satisfied the target strength.

Table 1: Mix design proportion (Average Strength= 25 MPa)

Material	Dolomite	Sand	Cement	Water
Mix Proportion (Kg/m ³)	898	863	384	230

The specimen's main longitudinal bottom and secondary top reinforcement high grade deformed steel bars. These bars applied to tension test and give 360MPa yield stress. Structural steel I sections for shear heads made from steel with nominal yield stress equal to 300 MPa.

2.2. Specimens Details

All tested flat slabs with overall thickness "h" equal to 150 mm and span equal 2000 mm in both directions with clear spans between supported beams equal to 1800 x 1800 mm. A total of seven slabs with square and rectangle column heads, were tested under punching shear loading. The clear concrete cover used was 10 mm to the bottom face of all test specimens. All slabs were reinforced with bottom longitudinal steel bars mesh $\Phi 18@100\text{mm}$ and top mesh with $\Phi 10@200\text{mm}$. All columns were reinforced with four longitudinal steel bars $\Phi 18$ and confined with $\Phi 10@100\text{mm}$ bars as transverse reinforcements. Several variables including column aspect ratio, length of shear head arm from column face will be taken into consideration. Research program plans was divided in two groups. The first group deals with testing three specimens of flat slabs connected with square columns, one specimen without any shear head as a control specimen and the other two specimens reinforced by steel shear head sections which have lengths equal to 1.75h and 2.25h, respectively from column face. The second group deals with four specimens of flat slabs connected with rectangular columns. one specimen without any shear head as a control specimen and the other three specimens reinforced by steel shear head sections which have a length equal to 1.75h with two cut ends at angles 90 and 45 degrees, and the last one with length equal to 2.25h. The two specimens without any shear head reinforcement (control specimens) are shown in Figure (4-a) and Figure (4-b). Table (2) summarizes the general description of the test specimens.

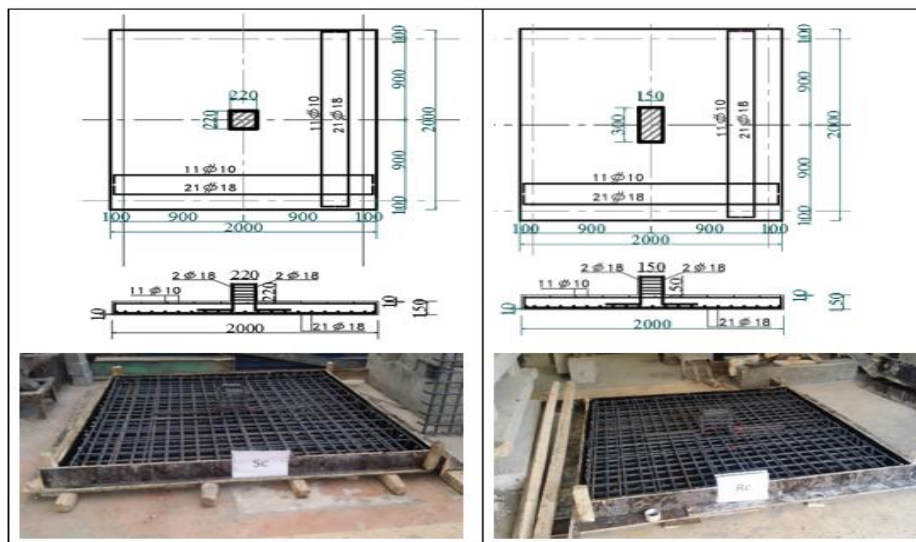


Figure (4-a): Flat slab specimen connected by square column [SC].

Figure (4-b): Flat slab specimen connected by rectangle column [RC].

Flat slab specimen connected with square column by embedded steel shear head sections between bottom and top reinforcement in which have a length equal to 1.75 from flat slab thickness named "S-L1-2" and its details shown in Figure (5).

Figure (6) shows specimen "S-L1-2" during preparing and placing of concrete in lab then use vibrator to compact concrete.

Table 2: General description of test specimens

Group	Specimen	Column aspect ratio	Column Dimensions	Shear head length	Remarks
Group (A)	SC	1	220*220	without	Control specimen
	S-L1-2	1	220*220	1.75 h	Cut end angle=90°
	S-L2-2	1	220*220	2.25 h	Cut end angle=90°
Group (B)	RC	2	150*300	without	Control specimen
	R-L1-2	2	150*300	1.75 h	Cut end angle=90°
	R-L1-2-45	2	150*300	1.75 h	Cut end angle=45°
	R-L2-2	2	150*300	2.25 h	Cut end angle=90°

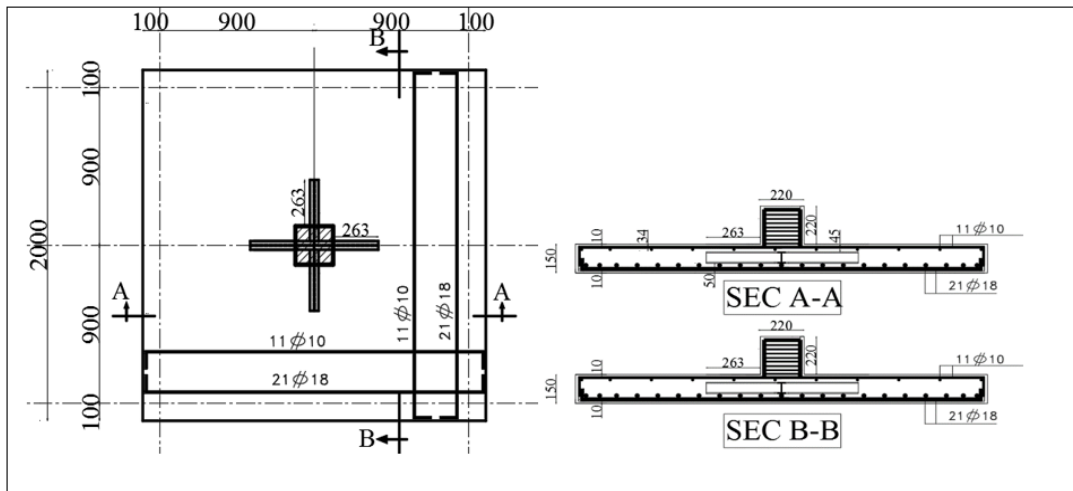


Figure (5): Reinforcement details of flat slab specimen "S-L1-2".



Figure (6): specimen "S-L1-2" during preparing and placing of concrete in lab.

Flat slab specimen in which connected with rectangle column by embedded steel shear head sections between bottom and top reinforcement in which have a length equal to 1.75h named "R-L1-2" and its details shown in Figure (7).

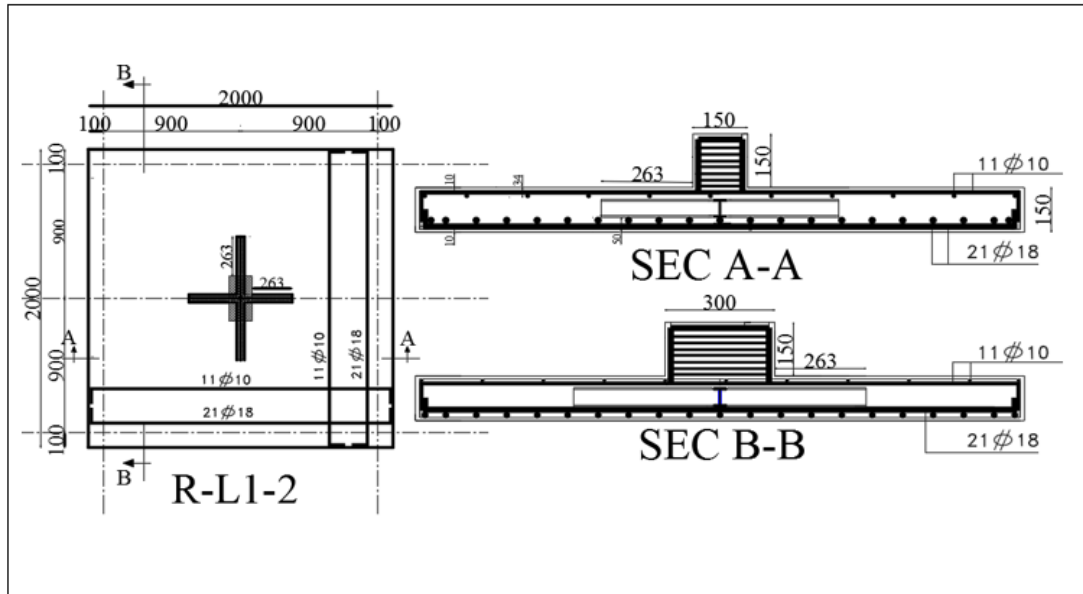


Figure (7): Reinforcement details of flat slab specimen "R-L1-2".

Figure (8) shows flat slab specimen "R-L1-2" during preparing and placing of concrete in lab then use vibrator to compact concrete.



Figure (8): Specimen "R-L1-2" during preparing and placing of concrete in lab.

2.3. Specimens Measuring Devices

Five "LVDTs" with accuracy of 0.01mm were used to measure the axial deformation. The axial deformation was measured at lower mid span of flat slab specimens, at L/8 and L/4 from mid span in two main directions. Figure (9) shows LVDTs locations on flat slab specimens in lab.

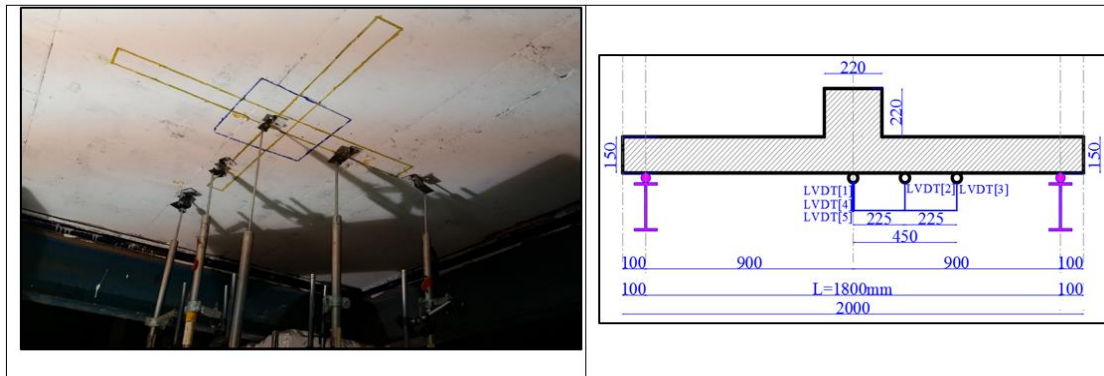


Figure (9): Locations of "LVDTs" on flat slab specimens.

Before casting the specimens, Electrical strain gauges with 10 mm length, 119.8 ± 0.2 Ohms' resistance, and gauge factor $2.11 \pm 1\%$ were used to measure the longitudinal strain of steel rebar at column face of flat slab specimen. The strain gauges fixed on rebar in the two main directions at column face as shown in Figure (10). The strain gauges were connected to a strain meter device with accuracy of 1×10^{-6} , and covered by a waterproof coating to protect them from water and damage during casting. In addition, the strains are recorded automatically using a data acquisition system.

Also, Electrical strain gauges with 10 mm length, 119.8 ± 0.2 ohms' resistance were used to measure shear strain in web and longitudinal strains of top and bottom flanges of steel shear head sections at $d/2$ and $0.75(L_v - c/2)$ from column face in an attempt for measure contribution of shear heads in punching shear and also to know however steel flanges reached to yielding or not, Figure (11) shows typical arrangement of strain gauges in web and flanges of steel shear head sections, then at every stage of loading, radial and tangential cracks were observed and marked.

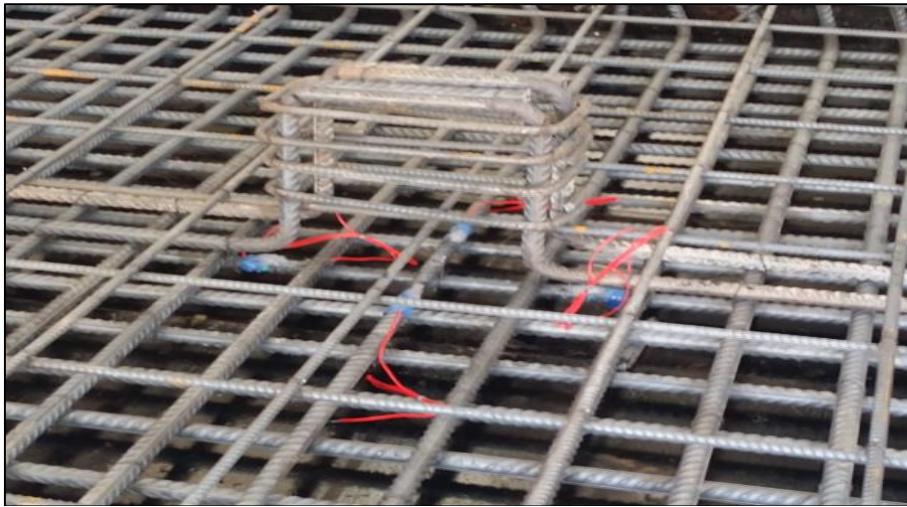


Figure (10): Locations of strain gauges fixed on rebars in the two main directions.

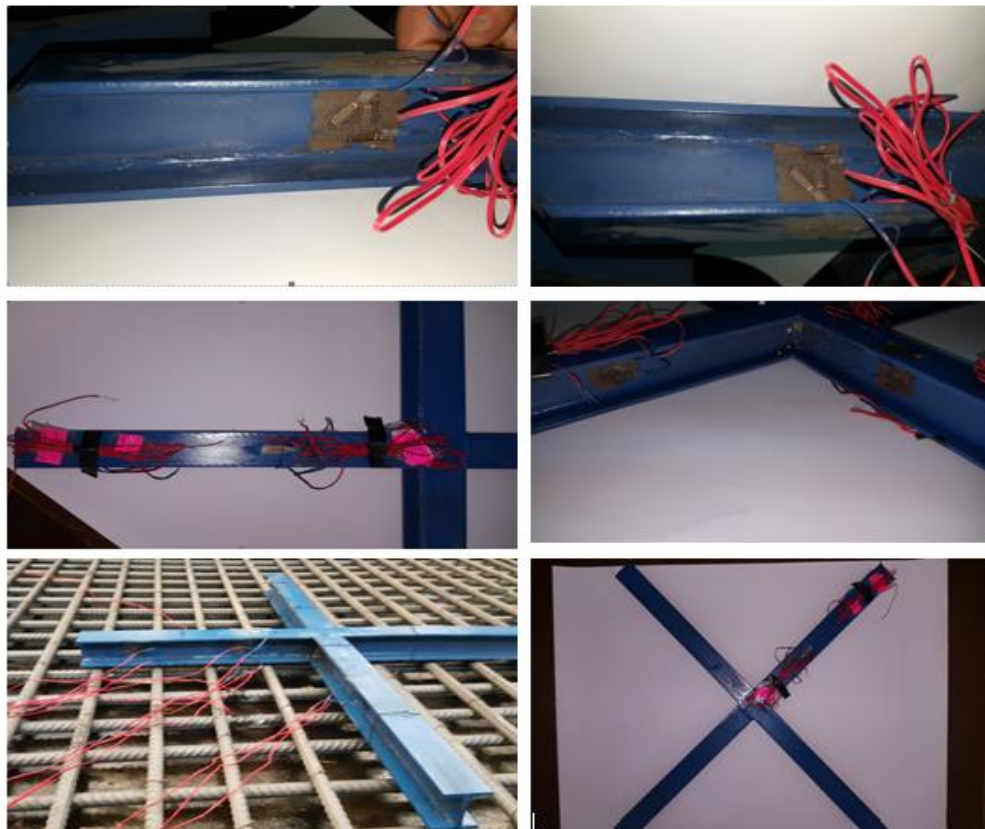


Figure (11): Typical arrangement of strain gauges in web and flanges of steel shear head.

2.4. Test Setup

The specimens were tested up to failure at laboratory of Housing and Building National Research Center (HBRC) using the testing frame as shown in Figure (12-a) and Figure (12-b). A load cell of 1000 KN capacity is used which is connected to a digital display unit. The column was directly loaded by jack through steel load plate and confined by steel jacket to avoid column failure before punching failure of the slab. The type of supporting system on the slab perimeter enables the specimen to rotate freely on their edges.

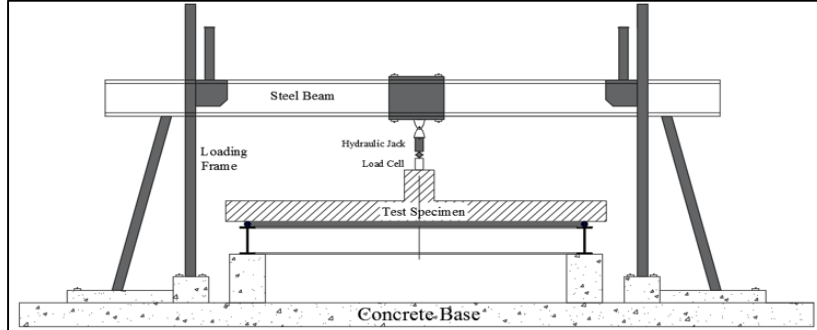


Figure (12-a): Layout of Test Specimens.



Figure (12-b): Typical test setup at "HBRC" lab.

III. EXPERIMENTAL TEST RESULTS

This section describes the experimental test results and discussion concerning ultimate loads versus axial deformations, strain in steel rebar, strain in steel shear heads and failure patterns.

3.1. Ultimate Loads versus axial deformation

The maximum experimental values obtained from all flat slab specimens were recorded and summarized in Table (3)

Table 3: Summary of test results

Group	Specimen	Ultimate load (kN)	Axial Displ. (mm.)	Failure Type	Max strain in steel rebar	Max Strain in shear head				
						Web			Flange	
						Vertical	Horizontal	diagonal	Top flange	Bottom flange
Group (A)	SC	473	10.95	Flexural punching	0.0022	----	----	----	----	----
	S-L1-2	556	11.9	pure punching	0.0024	-0.0001	-0.0003	+0.0006	-0.0006	+0.001
	S-L2-2	580	12.5	pure punching	0.0029	-0.00015	-0.00035	+0.0007	-0.001	+0.0015
Group (B)	RC	468	11.25	Flexural punching	0.0018	----	----	----	----	----
	R-L1-2	557	12.5	pure punching	0.0024	-0.0001	-0.00028	+0.0006	-0.0005	+0.001
	R-L1-2-45	516	11.3	pure punching	0.0025	-0.0001	-0.00026	+0.0005	-0.0006	+0.001
	R-L2-2	582	13.2	pure punching	0.0026	-0.00016	-0.00038	+0.0006	-0.001	+0.0014

For flat slab specimens which connected by square column (SC, S-L1-2 and S-L2-2), the relation between load and vertical displacement for all LVDTs locations at the bottom surface of flat slab specimen were

drawn on the same graph as shown in Figures (13) for control specimen. Figure (14) shows the load displacement diagram for all LVDTs of specimen (S-L1-2).

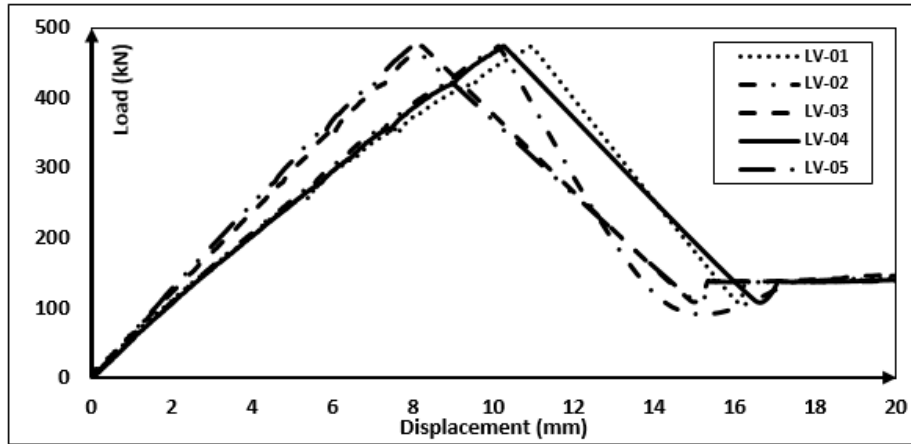


Figure (13): Load displacement diagram at LVDTs locations for control specimen [SC].

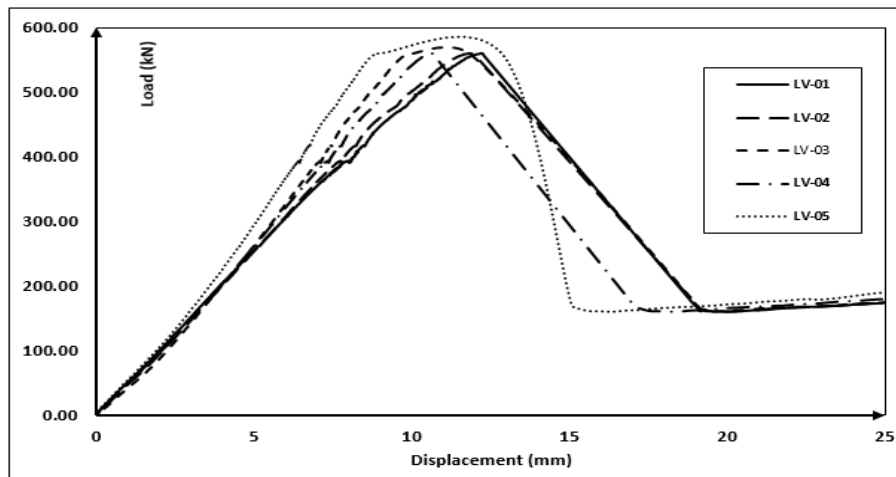


Figure (14): Load displacement diagram at LVDTs locations for specimen [S-L1-2].

Based on square specimen's results, the effect of using shear head reinforcement improved the punching shear capacity and ductility of slabs compared with control specimen. Figure (15) shows load displacement diagram for the three square specimens at LVDT (1) which was fixed at mid area of flat slab specimens. From this curve noting that there is an improvement in the value of the punching shear force of specimen S-L1-2 with percentage equal to 18.4% compared with control. Also, specimen S-L2-2 has an improvement ratio equal to 22.6% and 4.2% compared with control specimen and S-L1-2 respectively.

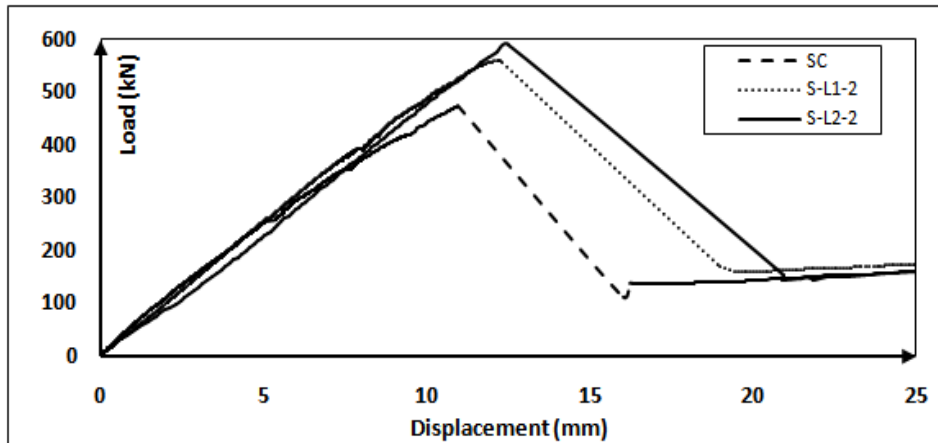


Figure (15): Load displacement diagram at control LVDT [1] for specimens which connected by square columns "SC, S-L1-2&S-L2-2".

For flat slab specimens which connected by rectangle columns (RC, R-L1-2, R-L1-2-45 and R-L2-2), the relation between load and vertical displacement for all "LVDTs" fixed on the control specimen were drawn Figures (16). Figure (17) shows the load displacement diagram for specimen (R-L1-2).

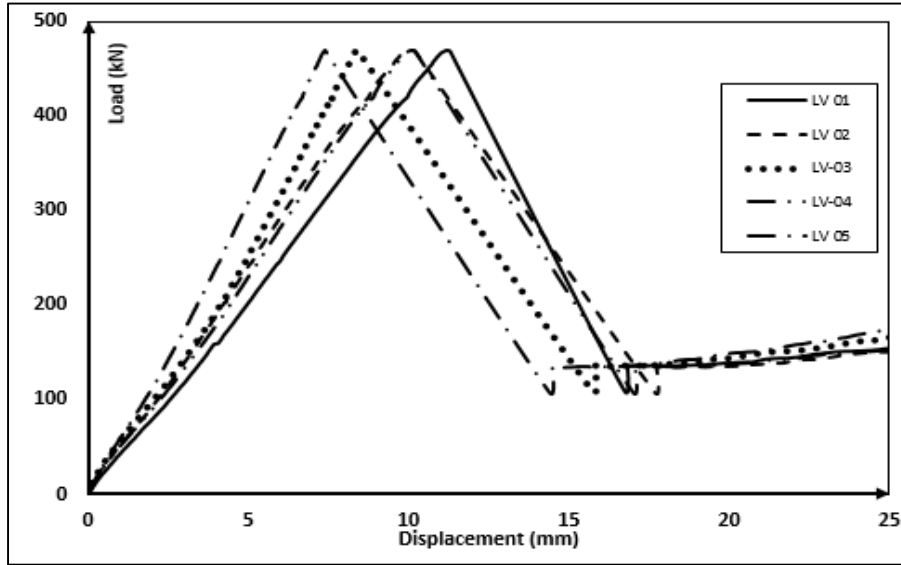


Figure (16): Load displacement diagram at LVDT locations for specimen RC.

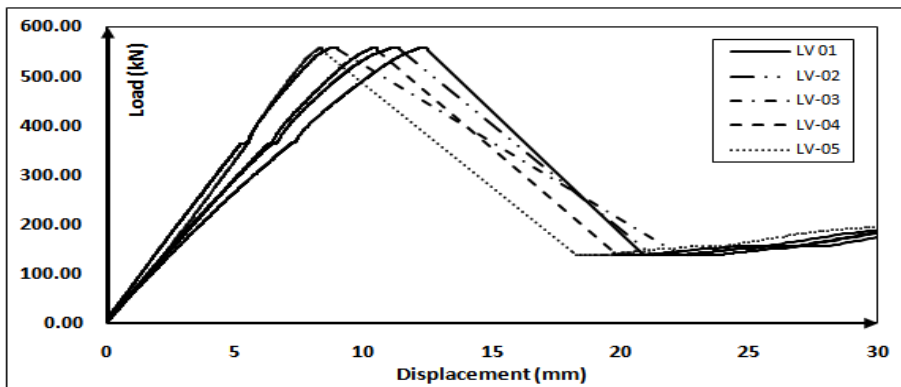


Figure (17): Load displacement diagram at LVDT locations for specimen R-L1-2.

Based on the results of rectangular columns specimens, the effect of using shear head reinforcement improved the punching shear capacity and ductility of slabs compared with control specimen. Figure (18) shows load displacement diagram for the three rectangular columns specimens at LVDT (1) which was fixed at mid area of flat slab specimens.

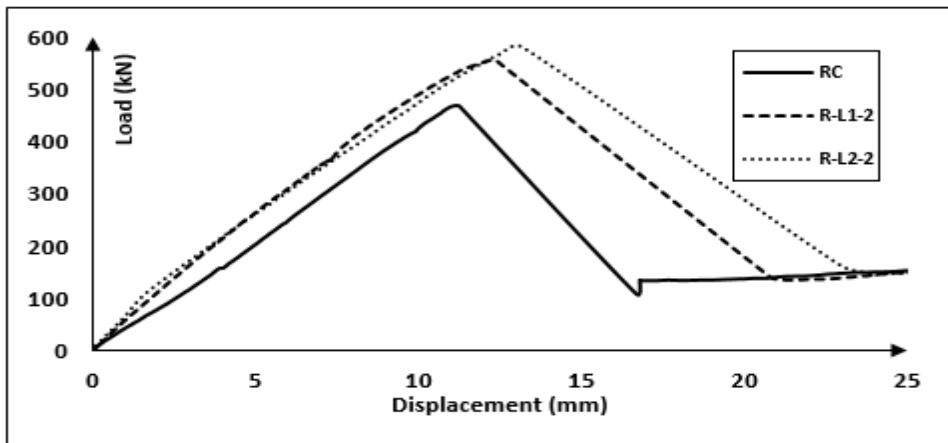


Figure (18): Load displacement diagram at control LVDT [1] for specimens which connected by rectangle columns [RC, R-L1-2&R-L2-2].

From this curve noting that there is an improvement in the value of the punching shear force of specimen R-L1-2 with percentage equal to 19% compared with control. Also, specimen R-L2-2 has an improvement ratio equal to 24% and 5% compared with control specimen and R-L1-2 respectively. By making a comparison between flat slab specimens which connected by square and rectangle column at the same length of shear heads observed that no significant change in punching shear and displacement values and these results ensure that flat slab specimens connected by a column with aspect ratio 2:1 approximately equal flat slab specimens connected by a column with aspect ratio 1:1.

Also, the results showed slight increase in the punching shear capacity and ductility between specimen with cut end angle equal 90 and 45 degrees at the same shear head length, as shown in Figure (19). It is recommended that, using steel shear head with cut end angle equal to 90 degrees gives better performance in punching shear capacity and displacement.

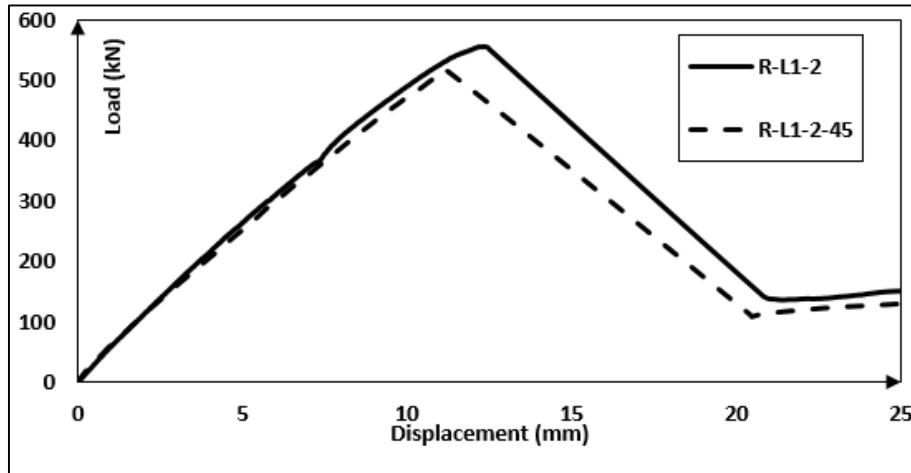


Figure (19): The difference between flat slab specimen by steel shear head with cut end angle equal to 90 and 45 degrees at the same shear head length.

3.2. Strain in steel rebar

In this part, longitudinal strains in steel rebar were observed. This observation indicated if the strain in steel rebars reached yield strain and consequently specify the type of failure whether pure punching failure or combination between flexural and punching failure. For flat slab specimens connected by square columns, the values of longitudinal strain in steel rebar on column face were observed, where the value of strain which makes steel rebar reaches to yielding is (0.0025). Figure (20) shows the relation between applied load of slab and longitudinal strain in steel rebar for control specimen (SC). The value of strain measured for the first steel rebar at column face (RFT1) is not the only value that indicates yielding occurrence. So in specimen "S-L2-2", strain gauges were fixed on the second and third steel rebar from column face (RFT2 & RFT3), and its results shown in Figure (21). Our point of view was confirmed by finding that the value of strain in other steel rebars(RFT2&RFT3) doesn't reach yielding.

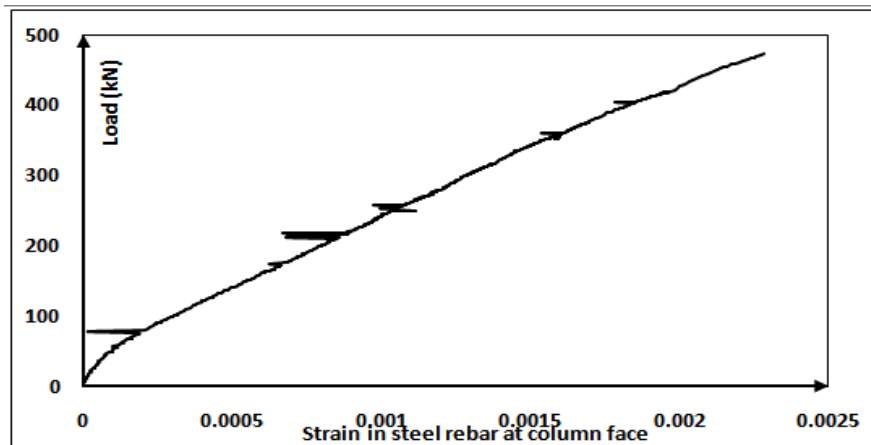


Figure (20): The relation between applied load of slab and longitudinal strain in steel rebar (RFT1) for control specimen (SC).

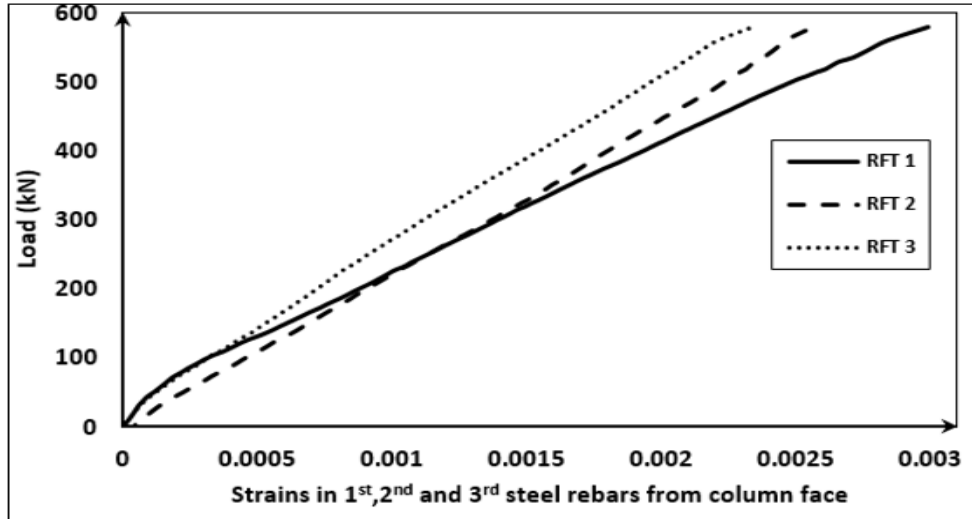


Figure (21): The relation between applied load of slab and longitudinal strain in steel rebar for specimen (S-L2-2).

For flat slab specimens connected by rectangle column (RC, R-L1-2, R-L1-2-45&R-L2-2), the values of longitudinal strain in steel rebar on short and long column directions were recorded for control specimen as shown in Figure (22). For specimen (R-L2-2), strain gauges were inserted in the second and third steel rebar parallel to the longitudinal direction of column (RFT2 &RFT3) as shown in Figure (23).

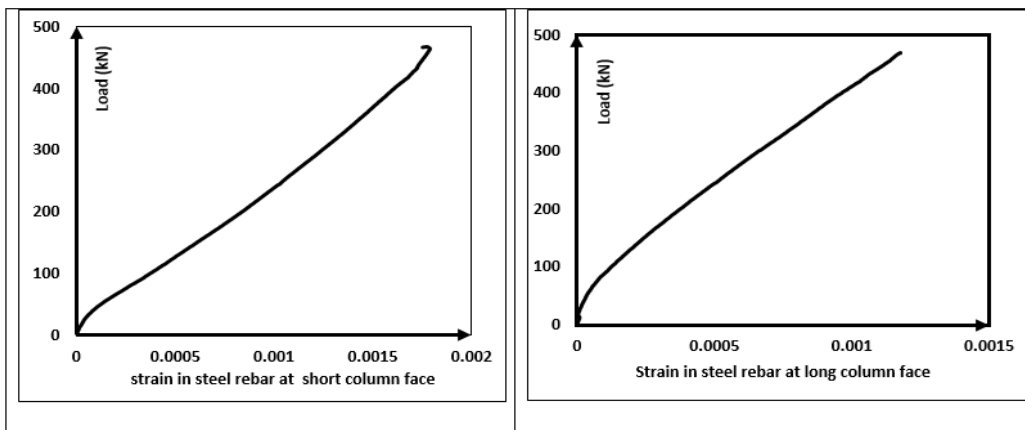


Figure (22): The relation between applied load of slab and longitudinal strain in steel rebar at short and long column face for control specimen (RC).

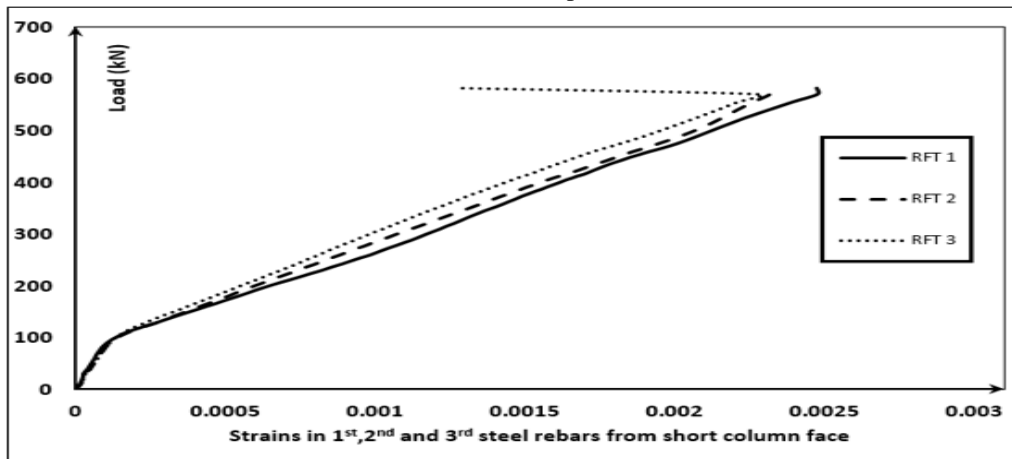


Figure (23): The relation between applied load of slab and longitudinal strain in steel rebar for specimen (R-L2-2).

3.3. Strain in steel shear head

A group of strain gauges were fixed in the web of shear head in three directions, vertical, horizontal and diagonal. Also, horizontal strains gauges were added in both flanges of the shear head in compression $d/2$ and $0.75(l_v - \frac{c}{2})$ from column face in which d is the slab thickness, l_v is length of shear head from center line of column, C is the square column dimension. The same set of strain gauges were also used for specimens with rectangular columns. The values of strain gauges were recorded in data logger and used to get the normal stresses and shear stresses in section web. Figure (24) shows directions of normal strains and stresses in the web of shear head. The following equations explain the mechanism of calculating contribution of shear heads in punching shear.

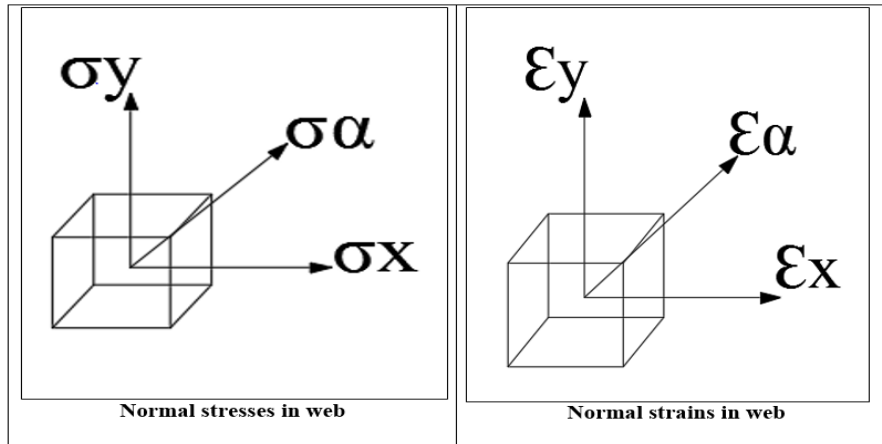


Figure (24): Normal strains and stresses in the web of shear head.

$$\sigma_{\alpha} = \frac{\sigma_x + \sigma_y}{2} + \frac{\sigma_x - \sigma_y}{2} \cdot \cos 2\alpha - \tau_x \cdot \sin 2\alpha$$

$$V = 4\tau_x \cdot A_{web}$$

The number 4 indicates the four sides of shear head.

3.5. Failure Patterns

The mode of failure of specimen "SC" was brittle since the failure occurred in concrete due to punching shear as shown in Figure (25). Figure (26) and Figure (27) shows the crack pattern and mode of failure at the top and bottom of specimens "S-L1-2" and "S-L2-2" respectively which give better performance more than control specimen "SC". It could be observed in specimen "S-L1-2" that the punching shear perimeter increased and exceed the end of steel shear head section also the punching shear perimeter increased in specimen "S-L2-2" but just reached the end of steel shear head section. The flat slab specimen which connected by rectangle column without shear head reinforcement "RC" have a brittle punching failure accompanied by some flexural cracks occurred in concrete as shown in Figure (28).



Figure (25): the crack pattern and mode of failure of specimen "SC".



Figure (26): The crack pattern and mode of failure at the top and bottom of specimen "S-L1-2"



Figure (27): The crack pattern and mode of failure at the top and bottom of specimen "S-L2-2"

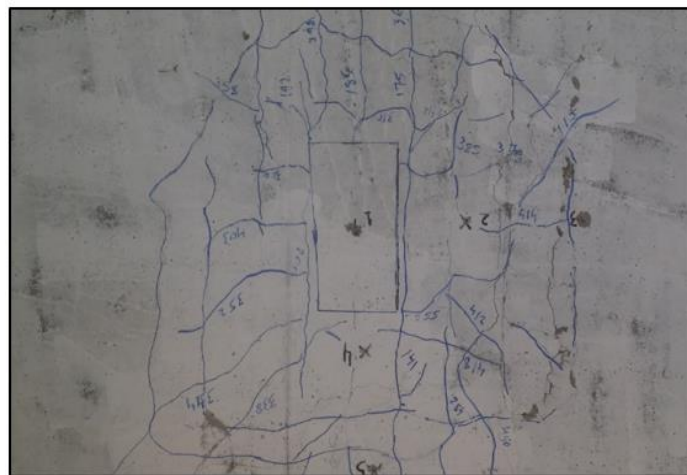


Figure (28): shows the crack pattern and mode of failure of specimen "RC".

Specimens "R-L1-2" and "R-L1-2-45" have the same length of shear head section but having a cut end angle equal to 90 and 45 degrees respectively, specimen "R-L1-2" give a better mode of failure more than specimen "R-L1-2-45", Figure (29), (30) shows the crack pattern and mode of failure at the top and bottom of the two specimens.



Figure (29): The crack pattern and mode of failure at the top and bottom of specimen "R-L1-2".



Figure (30): the crack pattern and mode of failure at the top and bottom of specimen "R-L1-2-45".

Specimen "R-L2-2" that contain steel shear head section with length 2.25h from short and long column face having the best mode of failure of all specimens that connected by rectangle column in which the resistance punching perimeter increased and reached to the edges of steel shear head section as shown in Figure (31).

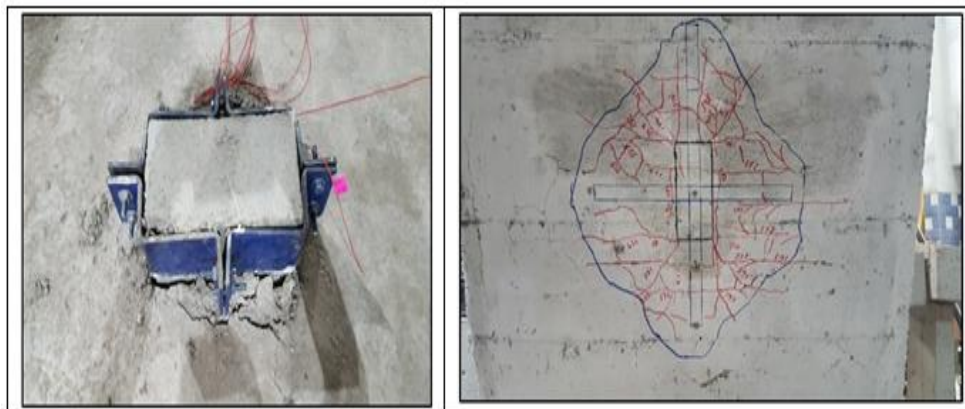


Figure (31): The crack pattern and mode of failure at the top and bottom of specimen "R-L2-2".

IV. ANALYTICAL PROPOSED EQUATION

4.1 ACI-318 Model

ACI [318R-14] is the only code which predict the resisting punching force of flat slabs with shear heads, to increase shear strength by steel I shapes (shear heads), the following steps should be followed:

1. Calculate total factored shear force $[V_u]$ according to the following equation:

$$V_u = W_{su} \cdot A \text{ where } A = (L \cdot B) - (a \cdot b) \dots\dots\dots [1]$$

Tributary areas and critical sections of shear as shown in Figure (32).

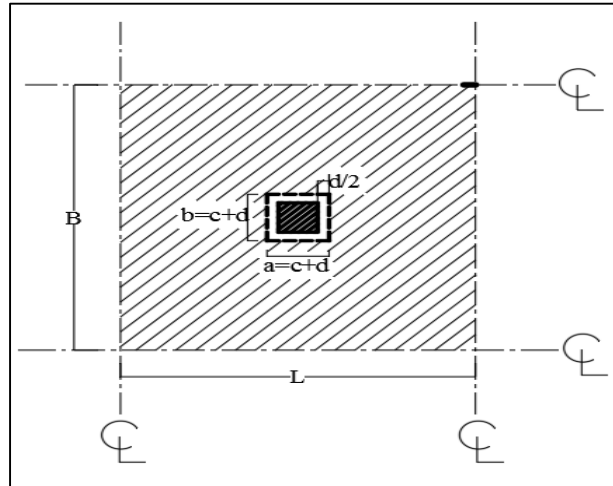


Figure (32): Tributary areas and critical section of shear.

2. Calculate shear strength (V_c) without shear reinforcement in which (V_c) is the smallest of the values obtained from equations. [2]- [4]:

$$V_c = 0.17 \left(1 + \frac{2}{\beta} \right) \lambda \sqrt{f_c'} b_o d \dots \dots \dots [2]$$

$$V_c = 0.083 \left(\frac{\alpha_s d}{b_o} + 2 \right) \lambda \sqrt{f_c'} b_o d \dots \dots \dots [3]$$

$$V_c = 0.33 \lambda \sqrt{f_c'} b_o d \dots \dots \dots [4]$$

Where β is the ratio of long side to short side of the column, $\lambda=1$ for normal weight concrete and $\lambda=0.85$ for semi light weight concrete, f_c' is the concrete cylinder compressive strength, $\alpha_s=40$ for interior column and b_o is the perimeter of the critical section.

3. Check the safety by comparing V_u with ΦV_c where $\Phi=0.75$
4. If the safety is not satisfied, it should be increase the shear strength by steel I shapes "Shear heads"
 - a. Check maximum shear strength permitted with steel shapes

$$V_n = \Phi (0.58 \sqrt{f_c'} b_{o1} d) \dots \dots \dots [5]$$

- b. Determine minimum required perimeter (b_{o2}) of a critical section at shear head ends with shear strength limited to

$$V_n = \Phi (0.33 \sqrt{f_c'} b_{o2} d) \dots \dots \dots [6]$$

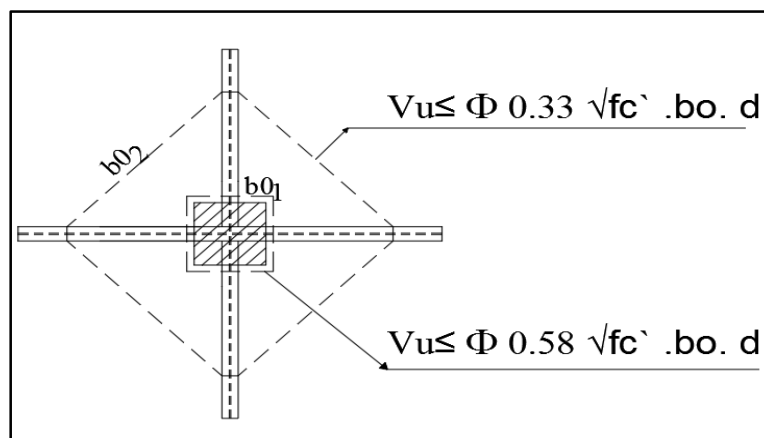


Figure (33): Allowable punching shear strength at different perimeters b_{o1} and b_{o2} , ACI [318R-14].

- b. Determine required length of shear head arm " L_v " to satisfy b_o

$$b_{o2} = 4\sqrt{2} \left[\frac{c}{2} + \frac{3}{4} \left(L_v - \frac{c}{2} \right) \right] \dots \dots \dots [7]$$

- c. To ensure that premature flexural failure of shear head does not occur before shear strength of slab is reached, the plastic moment required to ensure that the ultimate shear is attained as the moment strength of the shear head is reached should be calculated as follows.

$$\Phi M_p = \frac{V_u}{2n} \left[h_v + \alpha_v \left(L_v - \frac{c}{2} \right) \right] \dots \dots \dots [8]$$

Where:

M_p = plastic moment strength for each shear head arm

Φ = strength reduction factor for tension controlled member, equal to 0.9

n = number of shear head arms.

L_v = minimum required length of shear head arm.

h_v = depth of shear head cross-section.

α_v = the ratio between the flexural stiffness of each shear head arm and that of the surrounding composite cracked slab section of width $(c+d)$. [Assume $\alpha_v=0.25$]

- d. Check depth limitation of shear head web ($h_v < 70 t_w$)

- e. Determine location of composite flange of steel shape with respect to compression surface of slab in which compression flange must be located at 0.3 d .

4.2 Analytical Proposed Equation

Suggested crack path in flat slab specimens which contains shear head as it begins from column face with inclination angle equal to 45° and pass through the whole shear head length then it end at the bottom mesh with inclination angle 45°. Figure (34) shows the suggested crack path in flat slab specimens with shear head reinforcement.

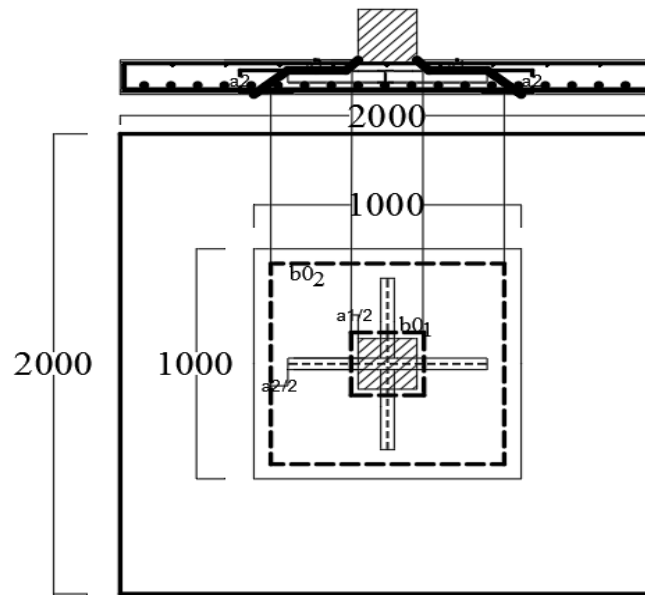


Figure (34): The suggested crack path in flat slab specimens with shear head reinforcement.

According to this crack path, the following equation is proposed to predict the punching shear capacity of flat slab with shear head:

$$V_u = v_1 * b_{01} * a_1 + v_2 * b_{02} * a_2 \dots \dots \dots [9]$$

Where:

V_u : punching shear capacity of slab with shear head reinforcement

v_1 : punching shear strength of slab at critical perimeter b_{01}

$v_1 = (0.58 \sqrt{f_c})$, assumed according to ACI [(318R-14)]

b_{01} : the first control perimeter at distance " $a_1/2$ " from column face

$b_{01} = 2[(c_x + a_1) + (c_y + a_1)]$

a_1 : distance from compression surface of concrete to top surface of steel I cross-section where, $[a_1 + a_2 = d]$

v_2 : punching shear strength of slab at critical perimeter $[b_{02}]$ may be assumed according to Dilger and Ghali (1981).

As the distance of the critical section from the column is increased, the length of the critical perimeter increases and for the same failure load, the shear stress resistance is decreased Sherif and Dilger (1996).

Dilger and Ghali (1981) who recommended that the shear stress resistance be expressed as a function of the ratio of the distance from the column face to the perimeter considered according to the following equation:

$$v_c = 0.17\sqrt{f_c'} \left(1 + \frac{2(4-\alpha_0)}{3\beta_c}\right) \geq 0.17\sqrt{f_c'} \dots\dots\dots [10]$$

Where $\beta_c = \frac{\text{long side}}{\text{short side}}$ of column and α_0 is the distance between column face and the critical section considered divided by d , which should not be taken smaller than 1. Figure (35) shows the shear stress resistance as a function of distance from column face divided by depth "d" in which the proposed equation by Dilger and Ghali(1981) reflects correctly the decrease of shear strength but assumes a constant strength for $\alpha_0 \geq 4$. Table 4 shows comparisons between the experimental and predicted ultimate capacities using ACI Committee 318, (2014) and proposal equation [20].

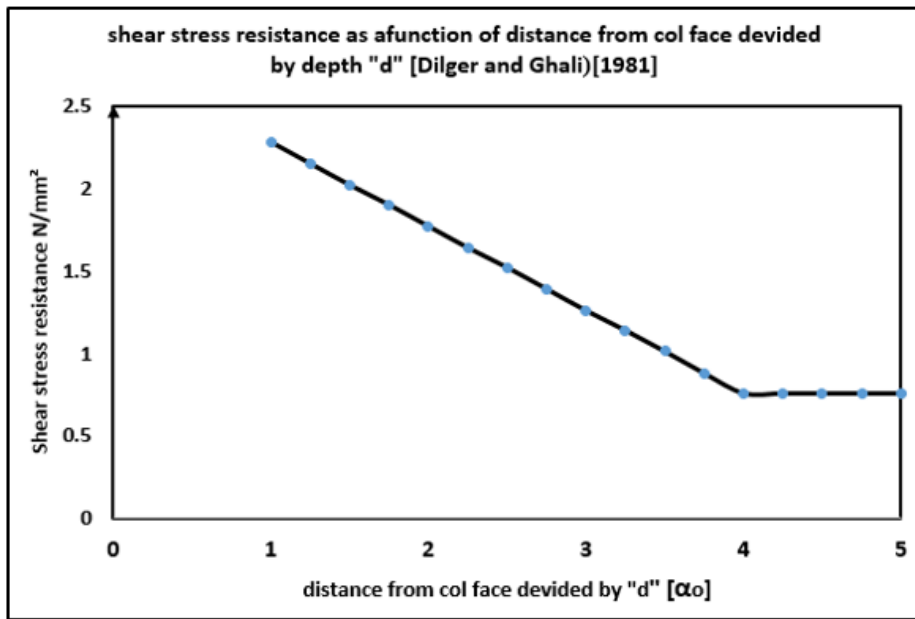


Figure (35): shows the shear stress resistance as a function of distance from column face divided by depth "d".

As can be seen from Table (4), the predicted punching shear capacities values from "ACI318R-14" code were more conservative than produced results values from the experimental program. The predicted values from the proposal equation have a good agreement compared with the experimental results.

Table 4: Comparison of experimental and predicted results

Specimen	V _u "exp" [kN]	V _u "ACI" [kN]	V _u "proposal equation"[kN]
SC	473.00	268.60	-----
S-L1-2	556.00	333.00	552.20
S-L2-2	580.00	398.00	557.40
RC	468.00	272.40	-----
R-L1-2	557.20	335.74	465.60
R-L1-2-45	515.90	335.74	453.6
R-L2-2	582.1	396.80	483.70

V. CONCLUSIONS

The research conducted showed that the using of embedded steel shear head sections has a good efficient in enhancing the ultimate punching shear capacity and ductility of flat slabs. Flat slab specimens which connected by a square column give almost same results with other specimens connected by a rectangle column with aspect ratio equal 2. Specific conclusions are as follows:

- 1- For flat slab specimens connected with square or rectangular columns having column aspect ratio 1 and 2 respectively, the enhancement in ultimate punching shear capacity was equal to 17.5% and 22.6% for shear head arms equal 1.75h and 2.25 h respectively.

- 2- shear head reinforcement which have cut end angle equal to 45 degrees have a lesser effect in enhancing punching shear capacity compared with similar one which have a cut end angle equal to 90 degrees.

The above findings are specific for flat slab specimens in which connected by columns which have aspect ratio equal 1 and 2 and for shear head arrangement which have 4 legs. General findings could be established by conducting future experiments with different column aspect ratios and different arrangement of shear heads. The method of calculating the use of shear heads was reviewed according to the American code and found that the method gives conservative values. The research proposed a new equation for calculating the punching shear capacity using shear heads. The proposed equation is based on calculation the punching shear capacity at the two proposed critical perimeters and calculate the length of shear heads used. This equation differs from the equation of the American code in taking effect of changing column aspect ratio and the lack of punching shear strength with increasing length of shear heads. The results of the proposed equation were compared with the results of the empirical study and the American code method. Results were close to the experimental results within the limits of 3% and 15% of the flat slabs with square and rectangular columns respectively.

REFERENCES

- [1]. ACI Committee 318, (1977), "Building Code Requirements for Reinforced Concrete (ACI 318-77)," American Concrete Institute, Farmington Hills, MI, 103 pp.
- [2]. ACI 318M-2005. Building code requirements for structural concrete and commentary. Committee 318, Farmington Hills, Michigan, USA; (2005). 430pp.
- [3]. ACI Committee 318, 2011, "Building Code Requirements for Structural Concrete (ACI 318-11) and Commentary," American Concrete Institute, Farmington Hills, MI, 503 pp.
- [4]. ACI Committee 318. 2014 "Commentary on Building Code Requirements for structural Concrete (ACI 318 R-14)." American Concrete Institute. Farmington Hills, MI,48331.
- [5]. Alaa G. Sherif and Walter H. Dilger (1996). "Critical review of the CSA A23-3-94 Punching shear strength provisions for interior columns", *Can.J.Civ.Eng.*23:998-1011(1996).
- [6]. CORLEY, W. G. & HAWKINS, N. M. (1968) Shear head Reinforcement for slabs. *ACI Journal*, October 1968, 811-824.
- [7]. Dan vasilBompa and Traian. Proceedings fib Symposium PRAGUE (2011) ISBN 978-80-87158-29-6 Session 1-4: New Model Code.
- [8]. Dilger, W.H., and Ghali, A. (1981), Shear reinforcement for concrete slabs *ASCE Journal of the structural divisions*, 107 (ST 12): 2403-2420.
- [9]. Hawkins, N. M., and Corley, W. G., (1974), "Moment Transfer to Columns in Slabs with Shear head Reinforcement," *Shear in Reinforced Concrete*, SP-42, American Concrete Institute, Farmington Hills, MI, Jan., pp. 847-880.
- [10]. Luca Tassinari, Stefan Lips, etc. Fib Symposium PRAGUE (2011) Session 2B-5: Construction Technology.
- [11]. Ospina C.E., Alexander S.D.B., and Cheng J.J.R. (2003). "Punching of Two-Way Concrete Slabs with Fiber-Reinforced Polymer Reinforcing Bars or Grids", *ACI Structural Journal*, V.100, No.5, September-October 2003, PP.589-598.

*Mohamed Badawy. "Punching Shear Resistance of Flat Slabs By Shear Heads." *International Journal Of Engineering Research And Development*, vol. 13, no. 11, 2017, pp. 47–65.